Water Air Soil Pollut (2025) 236:180
https://doi.org/10.1007/s11270-025-07809-2

Exploring Construction and Demolition Waste as a Sustainable Adsorbent for Efficient Removal of AB113 Dye from Aqueous Solutions

Brahim Arhoun · Maria del Mar Cerrillo-Gonzalez · Maria Villen-Guzman · Juan Manuel Paz-Garcia · Jose Miguel Rodriguez-Maroto

Received: 18 October 2024 / Accepted: 7 February 2025

Abstract An innovative approach to the treatment of textile wastewater by utilizing fine fractions of construction and demolition waste (CDW) as a cost-effective adsorbent is presented in this work. Through batch experiments, the impact of key parameters on the adsorption process was explored, identifying optimal conditions: natural pH, adsorbent dosage (S/L) of 20 g L^{-1}, and temperature of 20 °C. The characterization of CDW was performed using ICP, BET, FTIR, SEM–EDX, XPS, and XRD. The kinetics of adsorption were effectively described by the Elovich model, while equilibrium adsorption data showed good agreement with the Freundlich model. The maximum monolayer adsorption capacity for acid blue AB113 dye on CDW obtained from Langmuir isotherm was 89.52 mg g^{-1}. Thermodynamic analysis indicated an exothermic and feasible nature of the adsorption process. The results of this study highlight the potential use of fine CDW as a promising adsorbent to remove acid blue113 dye from textile wastewater.

Highlights

- Valorization of fine particles from construction waste as a circular economy strategy.
- Characterization of construction waste using ICP, BET, FTIR, SEM–EDX, XPS, and XRD.
- Construction and demolition waste used as an adsorbent material.
- The treated effluent meets regulatory standards for industrial wastewater discharge.

Keywords Fine construction wastes · Dye removal · Sustainable recycling · Circular economy · Cost-effective adsorbents

1 Introduction

Synthetic dyes are synthetic aromatic compounds widely used in various industries such as textile, leather, paper, and plastic. Annually, the production of commercial dyes exceeds 105 types, amounting to a staggering 7 million tons, with azo dyes alone constituting 60–70% of this output (Jain & Gogate, 2017;

Supplementary Information The online version contains supplementary material available at https://doi.org/10.1007/s11270-025-07809-2.

B. Arhoun · M. Cerrillo-Gonzalez (✉) · M. Villen-Guzman · J. Paz-Garcia · J. M. Rodriguez-Maroto
Chemical Engineering Department, Faculty of Sciences, University of Málaga, Málaga, Spain
e-mail: mcerrillog@uma.es

B. Arhoun
Laboratory of, Water, Studies and Environmental Analysis, Abdelmalek Essadi University, Tetouan, Morocco

Published online: 25 February 2025

Pai et al., 2021; Reza Samarghandi et al., 2020). However, the widespread use of dyes in industrial processes leads to the generation of vast quantities of wastewater, posing significant threats to both human health and the environment (Repon et al., 2024).

The textile sector utilizes substantial quantities of dyes, about 54%, and is one of the most polluting industries, which generates a significant volume of dye-containing wastewater (Değermenci et al., 2019; Hajjaji et al., 2016). Annually, more than 10^5 tonnes of azo dyes are consumed in the textile industry, with effluents containing around 10–15% of the total (Lee et al., 2016), and their concentrations in wastewater range from approximately 10–200 mg L^{-1} (Khalilzadeh Shirazi et al., 2020). In addition, dyeing and finishing operations in the textile industry consume about 1 m^3 of water per ton of cloth processed (Garg et al., 2004; Mohan et al., 2001; Patel, 2018). Every year, around 280,000 tons of dyestuff are released from various industry sources (Zewde et al., 2019). Chromophoric groups characterize the dyes, e.g., C-NH, =C=O, -CH=N-,—N=N-, C-S in their structure (Islam et al., 2021). Aromatic rings in the azo dyes are largely non-biodegradable (Shirzad-Siboni et al., 2014). Additionally, wastewater containing dyes is carcinogenic and toxic, posing threats to human health and aquatic ecosystems at low levels (Asgari et al., 2020; Esteban-Arranz et al., 2021; Prajapati & Mondal, 2020).

Acid blue 113 (AB113) dye is extensively used in textile industries, especially in the dyeing process (Lee et al., 2016; Ooi et al., 2017). Due to its high stability, non-biodegradability, and toxicity, removing these compounds from textile wastewater poses significant challenges (Reddy et al., 2022). Wastewater containing this dye can lead to increased biological oxygen demand, chemical oxygen demand, and water colour intensity (Lee et al., 2016; Reza Samarghandi et al., 2020). Additionally, it can diminish sunlight transmission, thereby slowing photosynthesis rates in aquatic ecosystems (Değermenci et al., 2019; Prajapati & Mondal, 2020; Wong et al., 2020). Hence, selecting an appropriate technology for treating dye-containing wastewater before discharge is crucial.

Several biological, chemical, and physical treatments are used for dye removal from industrial wastewater (Solayman et al., 2023). Biological methods, which use microorganisms like bacteria, fungi, and algae, are eco-friendly, cost-effective, and require fewer chemicals. However, they are time-intensive, pH-sensitive, and often ineffective against non-biodegradable dyes (Kishor et al., 2021). Chemical methods, such as coagulation-flocculation and advanced oxidation processes (AOPs), offer rapid treatment and can completely degrade dyes, but they are costly, generate secondary pollutants, and depend on specific conditions like pH and catalysts (Samsami et al., 2020). Physical methods, including adsorption and membrane filtration, are simple, flexible, and avoid chemical use, but they involve high operational costs, generate secondary waste, and may be limited in scalability (Akpomie & Conradie, 2020).

Adsorption, categorized as a physical process, has emerged as a highly effective alternative for wastewater treatment. This approach presents notable benefits, such as its remarkable efficiency, low economic cost, ready availability, cost-effectiveness, and straightforward operation (Esteban-Arranz et al., 2021; Prajapati et al., 2020; Uddin, 2017). Activated carbon is widely recognized as one of the most extensively used adsorbents globally. However, the high demand and cost of its production from non-renewable and expensive materials contribute to increased operational costs (Jain & Gogate, 2017; V. C. Silva et al., 2021). To overcome these limitations arising from the shortage, the search for other alternative adsorbents to replace activated carbon is of great importance. Clays are alternative candidates used as dye adsorbents because of their abundance, eco-friendliness, easy availability, high adsorptive properties, thermal stability, and relatively low cost (Khalilzadeh Shirazi et al., 2020; Márquez et al., 2021; V. C. Silva et al., 2021).

Furthermore, construction and demolition waste (CDW) accounts for a significant portion of global solid waste, with its generation exceeding 3 billion tons per year (Akhtar & Sarmah, 2018). In the European Union (EU), the total estimated quantity of mineral construction and demolition waste (excluding excavations) was 372 million tonnes in 2018. According to Eurostat, the annual production of mineral CDW in Spain stood at approximately 14.5 million tonnes, representing 10.5% of the total solid waste produced (Eurostat, 2018).

In accordance with the Waste Framework European Directive 2008/98/EC, the recycling target of 70% for CDW was required by 2020 (European Commission, 2008). However, the quantity of recycled waste falls significantly below this target, with only

approximately 50% being reused (European Commission, 2018). This discrepancy underscores the urgency of finding new CDW applications (Sormunen & Kärki, 2019). Currently, CDW finds practical use in civil engineering as filler material (Gálvez-Martos et al., 2018), backfilling in mines (Liu et al., 2020), or as filler material for beach regeneration (Arhoun et al., 2022). Nevertheless, the inert fraction of CDW also holds the potential for reuse as an adsorbent (Damrongsiri, 2017). Investigating the reutilization of fine CDW particles is crucial for the development of a circular economy strategy. Different studies have evaluated the use of CDW to adsorb different chemicals, such as phosphate (dos Reis et al., 2020), methylene blue dye (Domingues et al., 2024; Santos et al., 2024; H. J. B. da Silva et al., 2024) or ciprofloxacin (Caicedo et al., 2020). This work is focused on the study of CDW fine particles as an efficient and cost-effective adsorbent material to replace conventional adsorbents. To the best of our knowledge, the adsorption of AB113 dyes on fine CDW has not been previously reported.

This study aims to valorise fine particles of CDW waste for the dual purpose of waste volume reduction and industrial wastewater treatment, particularly targeting contaminants like AB113 dye. By conducting a comprehensive analysis of adsorption parameters (e.g., contact time, pH, dosage, and temperature) alongside kinetic, isotherm, and thermodynamic modelling, the study provides critical insights into the adsorption behaviour of AB113 onto CDW. The findings of this research demonstrate the potential for fine CDW particles to serve as an eco-friendly and efficient adsorbent, contributing to the sustainability of the waste management and industrial wastewater treatment.

2 Materials and Methods

2.1 Adsorbent Preparation

CDW was collected from ARECOSUR (Malaga, Spain), a recycling plant of CDW. In a previous study (Arhoun et al., 2022), raw CDW was treated for beach nourishment by a wet ball milling method. After that, the sample obtained was separated into three principal components: water, aggregate to use in the beach nourishment, and fine particles (< 2 mm) that were unfavourable to use in the beach nourishment. In this study, the fine particles were used as adsorbents of AB113 dye (Sigma-Aldrich). Following a screening process, the fine particles consisted of cement, sand, and lightweight concrete waste. Subsequently, the fine particles were sieved, and particles with sizes between 0.038 and 0.125 mm were selected for further experimentation.

2.2 Characterisation of Adsorbent

Characterisation of the solid before (CDW) and after the adsorption process (CDWA) was conducted using various analytical techniques. The determination of total metal content in CDW samples was carried out through microwave-assisted acid digestion, adhering to the guidelines of EPA method 3051A. Furthermore, the liquid fraction post AB113 adsorption on CDW was examined to assess the potential leaching of CDW elements into the aqueous medium. The elemental concentration in each supernatant was analysed using ICP.

To identify the functional groups present on the surface of the adsorbent before (CDW) and after the adsorption of AB113 dye (CDWA), the adsorbent underwent characterisation using Attenuated Total Reflection Fourier-transform infrared spectroscopy (FTIR-ATR). This evaluation was conducted utilising an FTIR spectrometer (Model Vertex70) equipped with the Golden Gate Single Reflection Diamond ATR System (Bruker, United States). A total of 64 scans were performed to record the spectra in absorbance mode across the range of 4000 to 500 cm^{-1} with a resolution of 4 cm^{-1}.

The surface characteristics and morphology of untreated CDW and any alterations post adsorption (CDWA) were examined using a Scanning Electron Microscope (SEM) (JEOL JSM-6490LV with Energy dispersive X-ray analyser). The Brunauer–Emmett–Teller (BET) method (Micromeritics ASAP 2020 model) was employed to determine the surface area, pore volume, and pore diameter of the CDW. Phase analysis was conducted using X-ray Diffraction (XRD, PAN analytical Xpert-Pro, Cu Kα: 1.5406 Å, 40 kV, 40 mA).

X-ray photoelectron spectra (XPS) were acquired using a Physical Electronics PHI 5701 spectrometer equipped with a multi-channel hemispherical electron

analyser manufactured by Physical Electronics, Inc., in Chanhassen, MN, USA.

2.3 Dye and Preparation of Solutions

The dye Acid Blue 113, with a molecular formula of $C_{32}H_{21}N_5Na_2O_6S$ and a molecular weight of 681.65 g mol $^{-1}$ (Colour Index Number 26360), was acquired from Sigma-Aldrich. The structural depiction of Acid Blue 113 can be observed in Fig. 1S (refer to supplementary materials). Initially, a stock solution containing 1000 mg L^{-1} of AB113 dye was prepared by dissolving the dye in deionised water. Subsequently, this stock solution was diluted to generate solutions with the desired dye concentrations. The pH levels of the solutions were regulated by the addition of 0.1 M HNO_3 (69% PanReac) or NaOH (Sigma-Aldrich) solutions.

The concentration of the AB113 dye was measured using a UV spectrophotometer (Shimadzu Model: UV 1280) at λ_{max} of 566 nm. Following centrifugation of the samples (Ortoalresa Model: Unicen 21) at 3500 rpm for 2 min to eliminate CDW particles, the resulting supernatants underwent filtration using a 0.45 mm filter and were examined with a UV/VIS spectrophotometer. The graph displaying absorbance against concentration was used to construct the calibration curve for AB113 dye. The correlation exhibited linearity within the 1 to 100 mg L^{-1} concentration range, with a coefficient of determination (R^2) of 0.9997.

2.4 Batch Adsorption Experiments

Batch experiments were conducted using continuous stirring on a rotary shaker operating at 200 rpm at 25 °C. The effect of contact time was assessed by submerging a specified quantity of adsorbent (10 g L^{-1}) in 50 mL of dye solution at the natural pH value (pH = 6.6) with no pH adjustments.

The impact of the initial pH was investigated across a range of values, from 2.5 to 12, while maintaining the optimal contact time of 180 min and utilising an adsorbent dose of 10 g L^{-1}. The influence of the adsorbent dose was examined within a range of 2 to 100 g L^{-1} at the optimal pH level (natural pH). The impact of the initial dye concentration was assessed at 25, 50, 75, and 100 mg L^{-1} levels using an adsorbent dose of 2 g L^{-1}. Furthermore, the effect of temperature on the adsorption processes was analysed across temperatures spanning from 20 to 40 °C.

Following a series of batch experiments, the residual solution underwent centrifugation at 3500 rpm for 2 min to remove suspended particles. Subsequently, the resultant supernatant was filtrated before being analysed using UV spectroscopy. Each test was conducted in duplicate under identical controlled conditions to ensure reproducibility, and the mean values were used to evaluate the kinetic, isotherm, and thermodynamic parameters.

The dye adsorption capacity and the percentage of dye removal were determined using the following equations:

$$q = \frac{C_i - C_f}{m} V \quad (1)$$

$$\% \text{ Colour removal} = \frac{C_i - C_f}{C_i} \cdot 100 \quad (2)$$

where q (mg g^{-1}) represents the amount of adsorbed dye, C_i (mg L^{-1}) is the initial dye concentration, C_f (mg L^{-1}) is the final dye concentration, V (L) is the volume of the dye solution, and m (g) is the mass of the adsorbent used.

2.5 Adsorption Equilibrium Isotherm and Kinetic Models

In this section, the adsorption equilibrium isotherm and kinetic models are presented (Tran et al., 2017). The equilibrium data were analysed using the Freundlich (Eq. 3) and Langmuir (Eq. 4) models to identify the best-fitting adsorption isotherm model.

$$q_e = K_f C_e^{1/n} \quad (3)$$

$$q_e = \frac{q_{m\_L}(k_L C_e)}{1 + (k_L C_e)} \quad (4)$$

where C_e (mg L^{-1}) is the equilibrium concentration, q_e (mg g^{-1}) is the amount adsorbed at equilibrium, K_f (L mg^{-1}) is the Freundlich constant, n is the Freundlich exponent, k_L (L mg^{-1}) is the Langmuir equilibrium constant, and q_{m_L} (mg g^{-1}) is the Langmuir maximum adsorption capacity.

The kinetics of AB113 adsorption onto CDW were assessed using the pseudo-first-order (Eq. 5),

pseudo-second-order (Eq. 6) and Elovich (Eq. 7) kinetic model. These models have been widely applied to mathematically describe the intrinsic kinetic adsorption constant (Tran et al., 2017; Wang & Guo, 2020).

$$q_t = q_e(1 - \exp(-k_1 t)) \tag{5}$$

$$q_t = \frac{q_e^2 k_2 t}{1 + (q_e k_2 t)} \tag{6}$$

$$q_t = \frac{1}{\beta_E} \ln(\alpha_E \beta_E t) \tag{7}$$

where q_t (mg g^{-1}) is the amount of dye adsorbed at time (t), k_1 (min^{-1}) is the pseudo-first-order rate constant, k_2 (g mg^{-1} min^{-1}) is the pseudo-second-order rate constant (g mg^{-1} min^{-1}), β_E (g mg^{-1}) is the Elovich constant and α_E (mg (g $min)^{-1}$) is the initial adsorption rate.

2.6 Evaluation of Model Performance

The adsorption parameters for the isotherms and kinetics models were determined using nonlinear regression. To identify the most suitable models and minimise prediction errors, the fit of the models to the experimental data was evaluated. This assessment was performed using the determination coefficient (R^2) and the root mean square error (RMSE) (Porter et al., 1999) calculated as follows:

$$R^2 = \frac{\sum_{i=1}^{N} \left(q_{e,model} - \overline{q}_{e,exp}\right)^2}{\sum_{i=1}^{N} \left(q_{e,model} - \overline{q}_{e,exp}\right)^2 + \left(q_{e,model} - q_{e,exp}\right)^2} \tag{8}$$

$$RMSE = \sqrt{\frac{1}{n} \sum_{I=1}^{N} \left(q_{e,exp} - q_{e,model}\right)_i^2} \tag{9}$$

where $q_{e,exp}$, $q_{e,model}$ and $\overline{q}_{e,exp}$ are the experimental, calculated using the models and average experimental adsorption capacity (mg g^{-1}), respectively, n is the number of data points, and p is the number of model parameters. For the best fitting of the experimental and calculated data, the determination coefficient (R^2) should be higher and close to 1, while RMSE errors should be minimized. Each experiment was carried out in duplicates. The mean values and standard deviation were reported in the graphs.

2.7 Adsorption Thermodynamics

The thermodynamic parameters, including the Gibbs free energy (ΔG°), enthalpy (ΔH°) and entropy (ΔS°), were determined following Eq. (10), Eq. (11) and Eq. (12) (Villen-Guzman et al., 2019), respectively:

$$\triangle G^\circ = -RT\ Ink_D \tag{10}$$

$$Lnk_D = \frac{\triangle H^\circ}{RT} + \frac{\triangle S^\circ}{R} \tag{11}$$

$$\triangle G^\circ = \triangle H^\circ - T \triangle S^\circ \tag{12}$$

where T (K) represents the temperature and k_D is distribution coefficient. The values of ΔH° (J mol^{-1}) and ΔS° (J mol^{-1} K^{-1}) were derived from the slope and intercept of the plot of Ln (k_D) versus 1/T.

3 Results and Discussion

3.1 Characterisation of Adsorbent

3.1.1 Isotherms of Nitrogen and Textural Properties

The physisorption isotherms of CDW and CDWA (before and after adsorption, respectively) are depicted in Fig. 2S. The specific surface area (S_{BET}) of both CDW samples was relatively low, with a value of 9.12 m^2g^{-1}, and they exhibited a total pore volume of 0.0183 cm^3 g^{-1}. Furthermore, the average pore size of 80.44 Å suggests the mesoporous nature of CDW according to the IUPAC classification (Liebau, 2003). For CDWA, the specific surface area was slightly lower at 8.15 m^2g^{-1}, with an average pore size of 85.93 Å and a total pore volume of 0.0175 cm^3 g^{-1}. Following the adsorption of AB113, only minor alterations in the CDW texture were observed. The limited porosity of CDW may indicate adsorption occurring primarily through functional surface groups.

3.1.2 Elemental Composition

The total content of different elements in CDW and the discharge of water is summarised in Table 1S. For CDW, Mg, Al, Si, K, Fe, Na and Ca were the most abundant elements, likely attributed to the presence

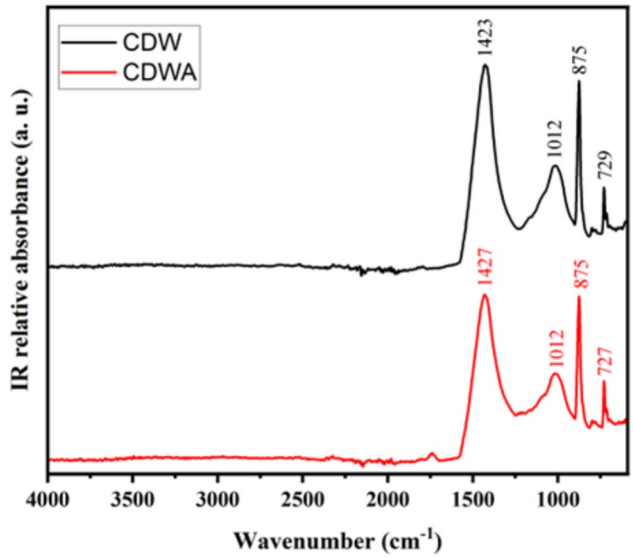

Fig. 1 ATR – FTIR spectra of CDW before and after adsorption. Before: CDW, After: CDWA

of cement and sand grains. Additionally, moderate concentrations of other elements, such as Ti, Mn, Sr, Ba and P were detected. Minor and trace elements were found in very low concentrations, some even below the detectable limit. As reported in our previous study (Arhoun et al., 2022), CDW is classified as an inert material, thus posing no risk when used as an adsorbent.

After the adsorption of AB113 dye on CDW, water discharge was analysed to assess the potential leaching of the CDW elements in the aqueous medium. Levels of Al, Fe, and Zn were far below the limiting value for discharging water (15 mg L^{-1} for Al, 10 mg L^{-1} for Fe, and 10 mg L^{-1} for Zn). Additionally, Ba, B, Cd, Zn, Pb, Ni, Cu, Cr, As, and Hg were not detected in water discharge. The remaining minor and trace elements were detected in very low concentrations. As can be seen, the concentration of metals and heavy metals in the water discharge consistently remained below the regulatory limit established by Spanish law for industrial wastewater discharge into public sanitation systems (BOE 2002).

3.1.3 X-ray Diffraction (XRD) Characterisation of the CDW Adsorbents

The mineralogical composition of CDW and CDWA was examined using XRD. In Fig. 3S, XRD analysis revealed a very prominent peak of dolomite, quartz, calcite and vermiculite, but with different intensity peaks (Bianchini et al., 2005; Pliatsikas et al., 2019). Dolomite and quartz were found in significant proportions, likely originating from cement/mortar. The presence of calcite could be primarily attributed to the carbonation of hydrated cement phases (Moreno-Pérez et al., 2018) and aggregates used in concrete manufacturing.

The mineralogical composition results of CDW obtained from XRD analysis align well with the chemical composition determined by ICP, confirming that the predominant elements in CDW are Mg, Al, Si, and Ca, which are essential constituents of dolomite, calcite, quartz, and vermiculite. The presence of various inorganic oxides can enhance the adsorption capabilities of CDW waste.

3.1.4 Fourier Transform Infrared (FT-IR) Spectroscopy

To understand the nature of the adsorption process of the AB113 dye, CDW and CDWA after adsorption were analysed using the ATR-FTIR spectroscopic technique. Results are presented in Fig. 1.

CDW- FTIR analysis before the adsorption reveals prominent absorption bands at 1423.1, 1012, 875, and 729 cm^{-1}. The presence of quartz and silicate phases in CDW is indicated by a band around 1012 cm^{-1}. The Si–O stretching band was observed for

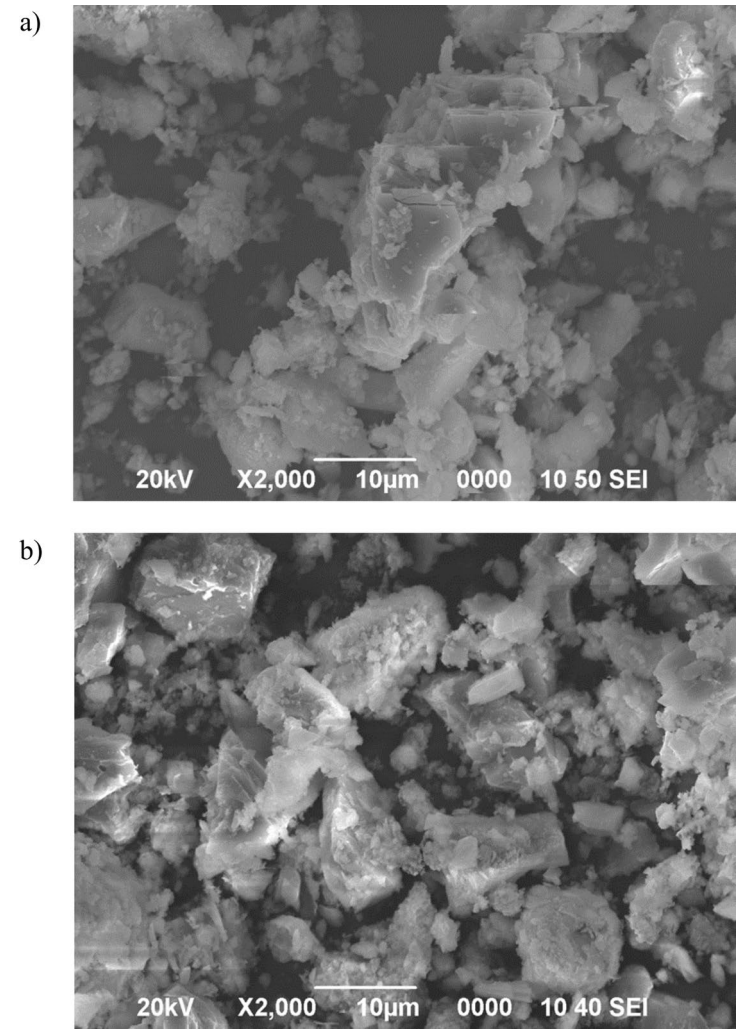

Fig. 2 SEM images of CDW (a), and CDWA (b)

Si–O vibration. Regarding the carbonate group's C-O vibration (at 1420 and 873 cm^{-1}) (Ooi et al., 2017), the bands at 1423.1, 875, and 729 cm^{-1} can be attributed to a different vibration of the carbonate unit: the first band associated with the asymmetric stretching vibration of the CO_3^{2-} group, the second associated band attributed to the out-of-plane bending vibration of the CO_3^{2-}group and the third associated band, generated by the in-plane bending vibration of the CO_3^{2-} group. These findings align well with the absorption frequencies reported in previous studies (Domingues et al., 2024; Santos et al., 2024).

After the adsorption of AB113 onto CDW, the ATR-FTIR spectrum revealed a shift and reduction in the intensities of certain functional group bands, suggesting the influence of AB113 dye-functional group interactions. These results indicated bonding between AB113 and CDW due to the adsorption or chemical reaction (A. A. Ahmad et al., 2007).

3.1.5 SEM–EDX of the CDW Adsorbent

The scanning electron microscopy (SEM) technique provides morphological and structural changes following the adsorption of AB113 dye. SEM images depicting CDW and CDWA before and after AB113 dye adsorption are presented in Fig. 2.

CDW display a mixture of irregular-shaped particles with a heterogeneous distribution of particle sizes and some layered structures containing particles of various sizes (Fig. 2a). The presence of dolomite,

Table 1 Chemical composition of CDW and CDWA (determined with EDX- normalised to 100)

Element	C (%)	O (%)	Mg (%)	Si (%)	Ca (%)
CDW	11.42	51.60	6.67	3.85	26.48
CDWA	15.23	54.05	6.30	3.52	20.91

identified as the main phase in CDW based on XRD, explains these layered structures. Khalilzadeh Shirazi et al. (2020) reported that dolomite possesses a structure composed of alternating layers of calcite and magnesite. Figure 2b highlights a significant alteration in the surface and morphology of CDW after the contact with AB113, indicative of AB113 dye adsorption.

The semi-quantitative analysis conducted on the surface of CDW and CDWA using energy dispersive X-ray spectroscopy (EDX) is presented in Table 1, indicating the main constituents as C, O, Mg, Si, and Ca. These findings align with the XRD analysis. Following adsorption, there is an observable increase in the C and O atomic percentages in CDWA, confirming the adsorption of AB113 dye onto CDW. As can be concluded, N and S were not detected by EDX semi-quantitative analysis due to their low percentages in AB113.

3.1.6 X-Ray Photoelectron Spectroscopy (XPS)

The surface chemical composition of CDW before and after adsorption with AB113 was analysed using XPS spectra (Fig. 4S), with results summarised in Table 2. The comprehensive spectral analysis of CDW reveals major elements such as C, O, Mg, Si, and Ca. As can be seen, C1s and O1s appear at high intensities, while minority elements such as Al and S were also detected. The O1s peak at 531.9044 eV is notably prominent, likely attributed to the carbon–oxygen and sulfur-oxygen bonds (O = C/O = S). The C1s signal at 284.7794 eV and 290.0294 eV were assigned to C–C or C = C in aromatic rings (Al-Musawi et al., 2022a, 2022b; Pai et al., 2021). The S2p in CDW shows a $S2p_{3/2}$ contribution at 169.9044 eV, indicating the presence of R-SO_3H or SO_4^{2-}. In summary, the results obtained from the XPS analysis are consistent with those from the XRD, EDX and FTIR analysis.

After the adsorption of Acid Blue 113 dye (molecular formula = $C_{32}H_{21}N_5Na_2O_6S_2$), the relative intensities of C1s and S2p increase for CDWA and N1s peak is detected. The increases in the intensity of the C1s peak at 284.83 eV can be attributed to the C = C bond in aromatic rings of the AB113 dye. In addition, the S2p core level for CDWA shows an increase in the intensity and a S2p3/2 contribution at 168.58 eV assigned to the presence of S(VI) as the sulfonic group of the dye (Jiménez-Jiménez et al., 2017; Mahapatra et al., 2018; Song et al., 2020). The peak detected at 399.93 eV after the adsorption of AB113 dye could be associated with the presence of azo-nitrogen (Seredych et al., 2014).

According to experimental results, the theoretical C/N atomic ratio is 6.4. The value of ΔC/N atomic ratio obtained after the adsorption of AB113 dye is 6.67, which is close to the theoretical value indicating the adsorption of AB113. However, Na was not detected, which could be associated with the dye anion (Jiménez-Jiménez et al., 2017) being taken up.

3.2 Effect of Contact Time and pH

The contact time and the pH value emerge as key parameters influencing the adsorption mechanisms. Figure 3a illustrates the impact of contact time on AB113 adsorption onto CDW. The findings indicate a rapid increase in dye removal, nearing 90% for a concentration of 100 mg L^{-1} within 1 h. As can be seen, the adsorption capacity (q) reaches over 50% of the equilibrium adsorption capacity within 3 min. Subsequently, a stable adsorption capacity is observed after 3 h. Consequently, a 3 h duration was selected in this study to attain equilibrium data for subsequent experiments, ensuring maximal dye adsorption. Initially, the increased removal rate can be attributed to the abundance of available vacant sites for AB113 dye adsorption. However, as these sites become occupied by dye molecules, the adsorption rate diminishes, reflecting a decline in available vacant sites. This phenomenon may also be influenced by repulsive forces between dye molecules adhered to the adsorbent surface and the bulk phases (Jain & Gogate, 2017).

The pH is essential in adsorption, influencing the adsorbent's surface chemistry and the dye molecule's ionising properties (Prajapati et al., 2020). Figure 3b illustrates the influence of pH on the adsorption of AB113 on CDW. It is evident that the adsorption

capacity remains relatively stable under acidic or neutral pH conditions. However, in a highly alkaline environment (pH value = 12), the adsorption capacity slightly decreases to 7.63 mg g^{-1} due to the acidic nature of AB113. This acidic character favours a predominant adsorption capacity at lower pH values.

The final pH values of the aqueous solution after AB113 adsorption on CDW were measured. Across initial pH value ranging from 2.5 and 12 (pH of the solution adjusted before adding the CDW), the resulting pH values are ranged between 9.22 and 11.83. It is due to the concrete waste, typically comprised by cement paste, and lightweight concrete, exhibits an alkaline pH with a notably high acid-neutralizing capacity (Damrongsiri, 2017). In this study, the dye exhibited its maximum adsorption capacity at an initial pH of 6.6, and all experiments were conducted under the natural pH conditions of the AB113 solution. This approach aligns with the methodology adopted by Jain and Gogate, (2017), who also employed a similar pH value.

3.3 Effect of Adsorbent Dosage

The influence of adsorbent dosage on the percentage removal of AB113 was examined by adjusting the S/L ratio from 1 to 100 g L^{-1} (C_i = 100 mg L^{-1} and natural pH), as depicted in Fig. 4. The increase in adsorbent dosage enhances dye adsorption, likely due to the enlarged surface area and availability of active sites for dye adsorption, thereby enhancing interactions between functional groups on the adsorbent surface (Chen et al., 2010).

According to the results, increasing the adsorbent dosage from 2 to 20 g L^{-1} resulted in a rise in dye removal from 66 to 96%. Beyond this dosage, there was no significant improvement in dye removal efficiency. An adsorbent dosage of 20 g L^{-1} was identified as the optimum dosage, beyond which further increases did not notably affect dye removal. At a dosage exceeding 20 g L^{-1}, the surplus of active adsorption sites and surface area of the adsorbent, coupled with the limited availability of dye molecules in the aqueous solution, resulted in no noticeable modification in the removal percentage. This could also be associated with the aggregation of fine CDW particles, decreasing the overall surface area. These findings are in agreement with prior studies (Al-Musawi et al., 2022a, 2022b; Ooi et al., 2017; Pai et al., 2021). Considering the significant dye removal at low adsorbent dosage, further experiments were conducted using an adsorbent dosage of 2 g L^{-1}.

3.4 Adsorption Kinetics

To analyse the kinetics of the adsorption process, the pseudo-first and the pseudo-second-order and Elovich models were fitted to the experimental data of acid dye AB113 adsorbed on CDW across various initial dye concentrations. The parameters for dye adsorption on the CDW surface, along with their corresponding R^2 and RMSE values, are presented in Table 3. The experimental data and kinetic models are presented in Fig. 5. The adsorption rate exhibited a rapid initial phase, reaching equilibrium within 60 min. As the initial dye concentration increased, the adsorption capacity (q_t) also increased, from 9.37 ± 0.41 at 25 mg L^{-1} to 28.72 ± 0.53 mg g^{-1} at 100 mg L^{-1}.

It can be seen that the calculated adsorption capacity obtained using the kinetic model parameters ($q_{e,\ model}$) was relatively close to experimental data ($q_{e,exp}$). To determine the best-fit model, R^2 and RMSE error functions were compared. The coefficient of determination (R^2) for the pseudo-first-order was lower than that obtained for the pseudo-second-order, and RMSE was higher than the pseudo-second-order. The Elovich equation, often used to describe the chemisorption of solutes on the adsorbent surface (Li et al., 2020; Nethaji & Sivasamy, 2011; Sun et al., 2015), showed a much higher R^2 and has a lower value of RMSE among the initial concentrations studied. Therefore, it can be concluded that the Elovich model is more suitable for describing the adsorption of AB113 on

Table 2 Content of elements on the surface of CDW and CDWA (in at. % from XPS analysis)

Sample	C	N	O	S	Mg	Al	Si	Ca
CDW	23.75	–	52.94	0.35	3.70	2.61	8.88	7.76
CDW-A	31.63	1.18	45.98	0.55	4.25	2	7.82	6.59

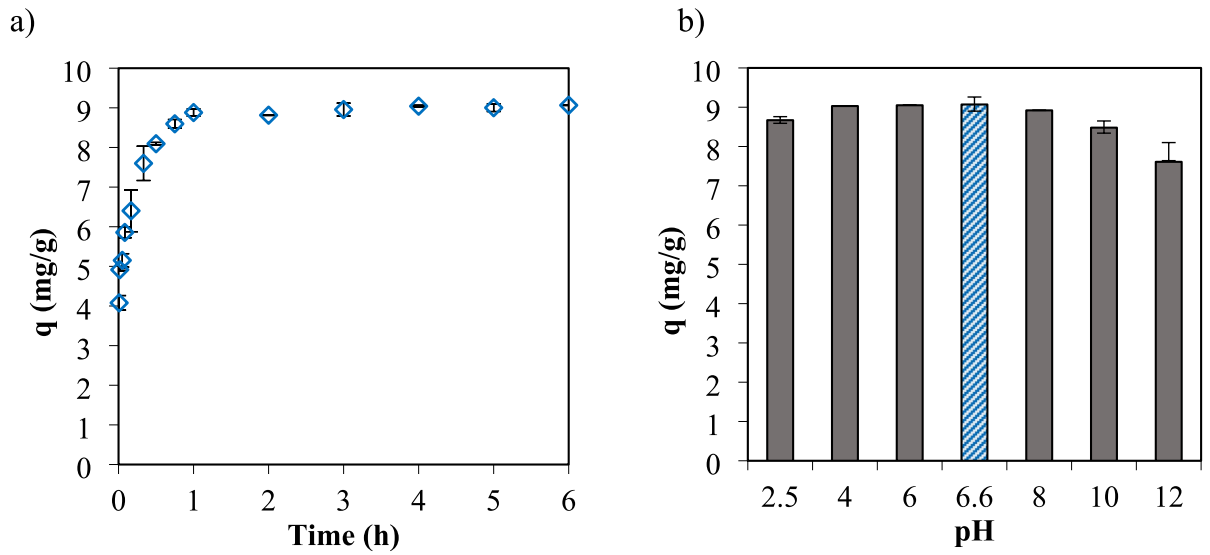

Fig. 3 A) Influence of contact time on adsorption of AB113 on CDW (natural pH; $C_0 = 100$ mg L^{-1}, S/L = 10 g L^{-1}), b) Influence of pH on adsorption capacity of AB113 on CDW. ($C_0 = 100$ mg L^{-1}, S/L = 10 g $L.^{-1}$)

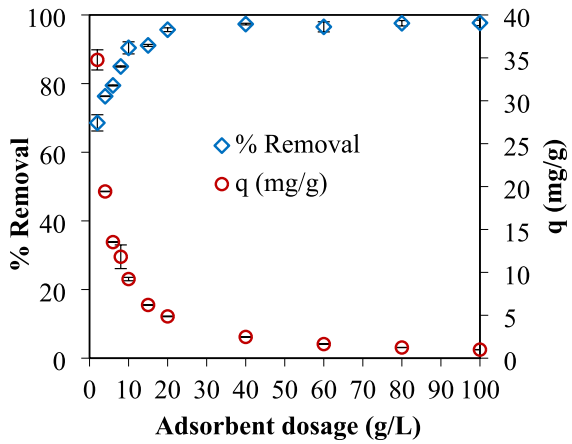

Fig. 4 Influence of adsorbent dosage on percentage removal and adsorption capacity of AB113 by CDW ($C_i = 100$ mg $L.^{-1}$, natural pH)

CDW, indicating that chemical adsorption also occurs in the process (Li et al., 2020).

To sum up, adsorption involves physical adsorption (functional groups) and chemical adsorption (Li et al., 2020). The parameters obtained from the Elovich model, presented in Table 3, show a change in these values with an increase in the initial concentration of AB113 dye. α_E and β_E are Elovich coefficients representing the initial adsorption rate and the desorption coefficient, respectively. The initial sorption rate, α_E, increases with the initial concentration, related to the increased driving force for mass and the concentration gradient for the migration of AB113 molecules (Debnath & Ghosh, 2008; Li et al., 2020). Although the initial sorption rate, α_E, decreases from an initial concentration of 75 mg L^{-1} to 100 mg L^{-1}, this might be attributed to the occupation of dye molecules on the surface and the subsequent agglomeration of dye molecules at the surface. The second parameter, β_E, is related to the extent of surface coverage and the activation energy for chemisorption (Aziam et al., 2017; Nethaji & Sivasamy, 2011). The reduction of this parameter (β_E) from 0.6604 to 0.2042 g mg^{-1} could be related to the decreased availability of surface area for the adsorption of AB113 (Li et al., 2020). The higher value of α_E compared to β_E suggests a higher adsorption rate than desorption, indicating the feasibility of the adsorption process (R. Ahmad et al., 2018).

3.5 Adsorption Isotherms

The experimental data were analysed by fitting them to the non-linear forms of the Freundlich and Langmuir isotherm models to determine the best fit among

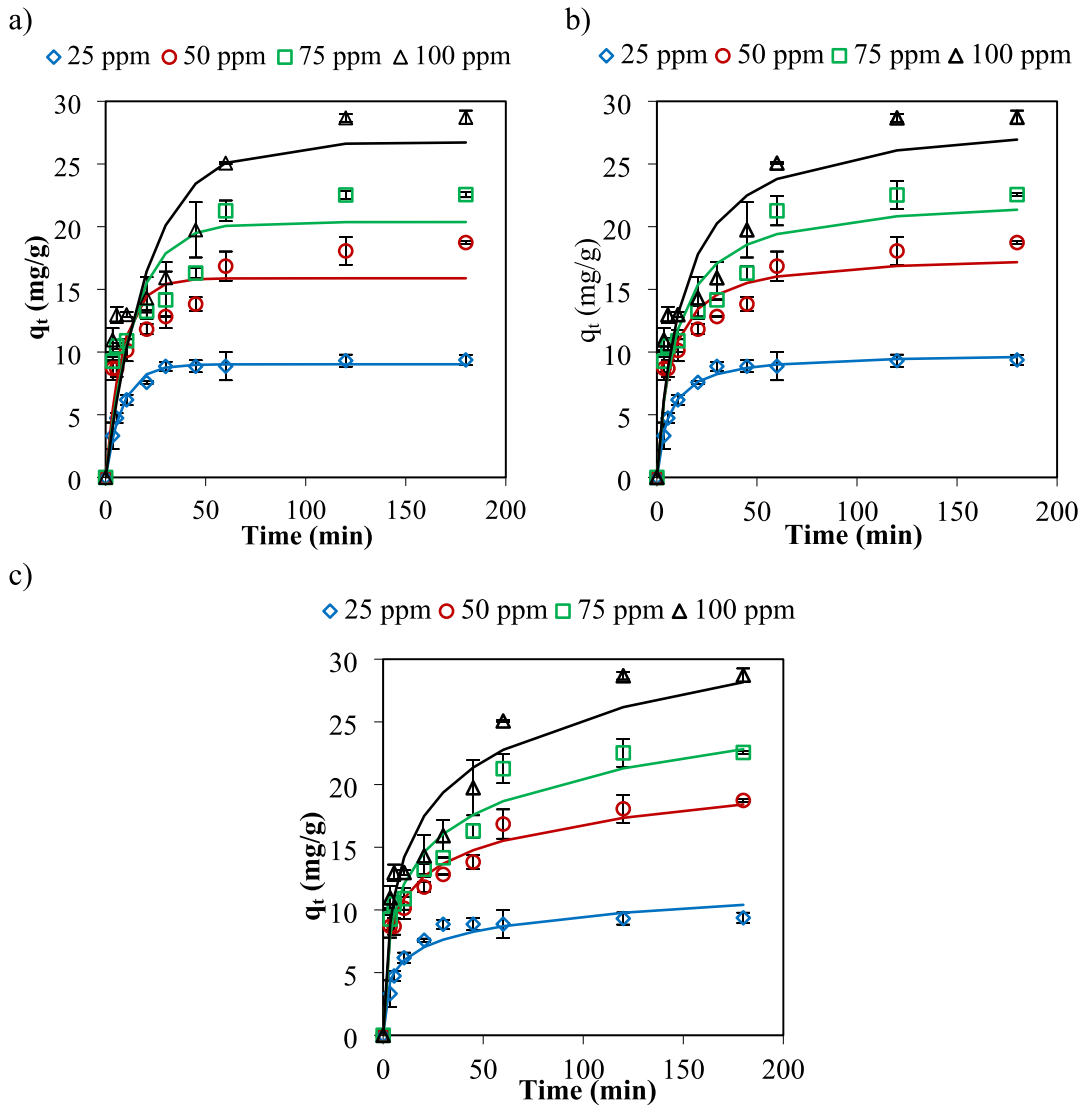

Fig. 5 Kinetic studies of AB113 dye adsorption. a) first-order model, b) second-order model and c) Elovich model. Points represents experimental data, continuous lines correspond to fitting curves for CDW adsorbent (natural pH, S/L = 2 g L^{-1})

the different models used (Fig. 6). The calculated parameters of the isotherm models, along with their corresponding R^2 and RMSE values, are presented in Table 2S.

Based on the correlation values obtained, it can be concluded that the Freundlich isotherm provides a better fit to the experimental data compared to the Langmuir model, as indicated by a higher R^2 value (0.9837) and lower RMSE value (2.7656). Additionally, the Freundlich parameter $1/n$ was found to be less than 1 ($1 < n < 10$), indicating favourable adsorption conditions or a chemisorption process (Damrongsiri, 2017; Sadeghi et al., 2015).

The values obtained for the $q_{e,model}$ using the Freundlich model closely match those obtained from experimental data, $q_{e,exp}$. These results can be explained by the heterogeneity of construction and demolition waste. The surface of CDW has different porosity and active sites with varying energies, which aligns well with the Freundlich model, assuming adsorption occurs on a heterogeneous surface. The monolayer adsorption capacity was determined from

Table 3 Kinetic parameters for adsorption of AB113 on CDW adsorbent

Kinetic model		AB113 concentration (mg L^{-1})			
		25	50	75	100
Pseudo first-order	k_1 (min^{-1})	0.1182	0.1176	0.0699	0.0466
	q (mg g^{-1})	9.3714	18.3717	22.5615	28.7256
	$q_{e,\ model}$ (mg g^{-1})	9.0253	15.8850	20.3688	26.7209
	R^2	0.9897	0.8259	0.8679	0.8627
	RMSE	0.3260	2.6293	2.9699	4.0437
Pseudo second- order	k_2 (g min^{-1} mg^{-1})	0.0163	0.0084	0.0047	0.0027
	q (mg g^{-1})	9.3714	18.3717	22.5615	28.7256
	$q_{e,\ model}$ (mg g^{-1})	9.9291	17.8049	22.4780	28.8513
	R^2	0.9935	0.9323	0.9162	0.8933
	RMSE	0.2527	1.5103	2.1604	3.1727
Elovich	α_E (mg (g $min)^{-1}$)	7.0746	15.8632	8.8188	8.4355
	β_E (g mg^{-1})	0.6449	0.3795	0.2646	0.2036
	R^2	0.9491	0.9772	0.9566	0.8913
	RMSE	0.8058	0.9334	1.6605	2.5718

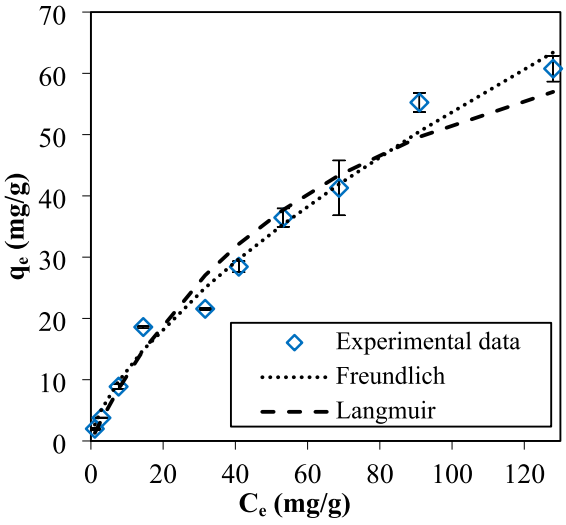

Fig. 6 Equilibrium adsorption isotherm for the adsorption of AB113 dye on CDW. (natural pH, S/L = 2 g $L.^{-1}$)

g^{-1}.

3.6 Effect of Temperature

The adsorption capacity experiences significant variations with temperature. From the plot of $ln\ K_D$ versus $1/T$, the thermodynamic parameters are evaluated, as presented in Table 4.

The negative values of $\Delta G°$ suggest that the adsorption of AB113 dye onto CDW is feasible and spontaneous. The negative enthalpy ($\Delta H°$) values suggest an exothermic process and the physical nature of the adsorption process. This phenomenon may be attributed to the weakening of the forces between the AB113 dye and the active sites on the adsorbent surface (Aziam et al., 2016; Yagub et al., 2014), or the tendency of AB113 dye molecules to transition from the solid phase to the bulk phase with increasing temperatures (Gupta et al., 2011; Jain & Gogate,

Table 4 Thermodynamic parameters for the adsorption of AB113 on CDW

Temperature (K)	ΔG° (kJ mol^{-1})	ΔH° (kJ mol^{-1})	ΔS° (kJ mol^{-1} K^{-1})
294.75	−3.14	−48.70	−0.018
298.65	−2.85		
302.75	−2.15		
308.75	−1.06		
313.65	−0.36		

the Langmuir model, yielding a value of 89.52 mg

Table 5 Comparison of Langmuir maximum adsorption capacity for the adsorption of acid blue AB113

Adsorbents	T (K)	q_m (mg g^{-1})	pH	References
Green synthesized Fe_3O_4 nanoparticles	303	138.89	2	(Pai et al., 2021)
Modified goat collagen fiber (PCMGCF),	299	31.52	4	(Mahapatra et al., 2018)
Mixed fish scales	30	145.3		(Ooi et al., 2017)
Commercial activated carbon	298	7.19	5	(Gupta et al., 2011)
Waste rubber tire	298	9.2	2	(Gupta et al., 2011)
Rubber tire activated carbon	298	83.3	3	(Shirzad-Siboni et al., 2014)
Overripe *Cucumis sativus*	303	52.20	2	(Lee et al., 2016)
Modified Fallen leaves of *Prunus Dulcis (SMPD)*	293	97.09	6.8	(Jain & Gogate, 2017)
Modified Fallen leaves of *Prunus Dulcis* (NTPD)	293	25.51	6.5	(Jain & Gogate, 2017)
Carpobrotus edulis plant	298	8.20	6.3	(Aziam et al., 2017)
Pillared porous phosphate heterostructure	298	65.92	6.5	(Jiménez-Jiménez et al., 2017)
Tribulus terrestris spent,	303	93	2	(Dhaif-Allah et al., 2020)
P(MMA)-g-TG/Betonite	298	46.51	8	(Sadeghi et al., 2015)
C-Fe_2O_3	298	128	3	(Al-Musawi et al., 2022a, 2022b)
CDW	298	89.52	6.5	This study

2017). The observed exothermic nature of the adsorption process aligns with findings in previous literature (Deniz & Saygideger, 2011; Errais et al., 2011; Gupta et al., 2011; Jain & Gogate, 2017; Ooi et al., 2017; Pai et al., 2021). Additionally, the negative $\Delta S°$ value indicated a decrease in randomness at the solid/solution interfaces during adsorption.

3.7 Comparison with Published Data

The adsorption of AB113 dye on various adsorbents reported in the literature is summarised in Table 5. The maximum adsorption capacity (q_m) obtained in this study under optimal conditions is compared with results obtained for other adsorbents at similar temperature values. The results indicated that the value of q_m is comparable to that of different adsorbents. Based on this comparison, it can be concluded that CDW without surface modification has a high potential to remove AB113 from textile wastewater.

4 Conclusion

CDW has been demonstrated to be a highly efficient adsorbent for removing AB113 from aqueous solutions. Several parameters have been identified to influence the adsorption capacity directly. The natural pH of the dye solution was determined as the optimal value for achieving maximum removal of AB113. The removal capacity increased with higher doses of the adsorbent and decreased with rising temperature. The Freundlich isotherm model was employed to characterise the adsorption of AB113 on CDW, revealing surface heterogeneity and favourable adsorption conditions. Additionally, the Elovish model showed an excellent fit with the kinetic data, indicating the energetically heterogeneous adsorption of AB113 onto the solid surface. The thermodynamic parameters confirm the exothermic and spontaneous nature of the adsorption process. Changes in the surface properties of CDW after adsorption further confirmed the binding of AB113 on CDW. These findings highlight the potential of CDW as a sustainable and effective solution for the removal of AB113 dye from aqueous solutions, contributing to the development of environmentally friendly wastewater treatment processes.

Acknowledgements The authors acknowledge the funding received from the UIA02–306 (BRICK-BEACH project) to the municipality of Vélez-Málaga (Spain). Funding for open access charge: Universidad de Malaga/CBUA.

Author Contribution **B. A.:** Writing – review & editing, Writing – original draft, Methodology, Investigation, Conceptualization, Formal analysis. **M.M.C.G**: Writing – original draft, Investigation, Formal analysis. **M.V.G:** Writing – review

& editing, Validation, Supervision, Methodology, Conceptualization. **J.M.P.G.:** Writing – review & editing, Validation, Supervision, Conceptualization**. J.M.R.M**: Writing – review & editing, Validation, Supervision, Conceptualization, funding.

Funding Funding for open access publishing: Universidad de Málaga/CBUA.

Data Availability All data generated or analysed during this study will be available upon request.

Declarations

Conflict of Interest The authors have no known competing financial interests, personal relationships, or any other conflict of interest that could have appeared to influence this research work.

References

Ahmad, A. A., Hameed, B. H., & Aziz, N. (2007). Adsorption of direct dye on palm ash: Kinetic and equilibrium modeling. *Journal of Hazardous Materials, 141*(1), 70–76. https://doi.org/10.1016/j.jhazmat.2006.06.094

Ahmad, R., Aslam, M., Park, E., Chang, S., Kwon, D., & Kim, J. (2018). Submerged low-cost pyrophyllite ceramic membrane filtration combined with GAC as fluidized particles for industrial wastewater treatment. *Chemosphere, 206*, 784–792. https://doi.org/10.1016/j.chemosphere.2018.05.045

Akhtar, A., & Sarmah, A. K. (2018). Construction and demolition waste generation and properties of recycled aggregate concrete: A global perspective. *Journal of Cleaner Production, 186*, 262–281. https://doi.org/10.1016/j.jclepro.2018.03.085

Akpomie, K. G., & Conradie, J. (2020). Advances in application of cotton-based adsorbents for heavy metals trapping, surface modifications and future perspectives. *Ecotoxicology and Environmental Safety, 201*, 110825. https://doi.org/10.1016/j.ecoenv.2020.110825

Al-Musawi, T. J., McKay, G., Rajiv, P., Mengelizadeh, N., & Balarak, D. (2022a). Efficient sonophotocatalytic degradation of acid blue 113 dye using a hybrid nanocomposite of CoFe2O4 nanoparticles loaded on multi-walled carbon nanotubes. *Journal of Photochemistry and Photobiology a: Chemistry, 424*, 113617. https://doi.org/10.1016/j.jphotochem.2021.113617

Al-Musawi, T. J., Mengelizadeh, N., Al Rawi, O., & Balarak, D. (2022b). Capacity and Modeling of Acid Blue 113 Dye Adsorption onto Chitosan Magnetized by Fe2O3 Nanoparticles. *Journal of Polymers and the Environment, 30*(1), 344–359. https://doi.org/10.1007/s10924-021-02200-8

Arhoun, B., Jiménez, C., Niell, F. X., & Rodriguez-Maroto, J. M. (2022). Investigating the physical and chemical characteristics of construction and demolition wastes as filler to regenerate beaches. *Resources, Conservation and Recycling, 179*, 106044. https://doi.org/10.1016/j.resconrec.2021.106044

Asgari, G., Shabanloo, A., Salari, M., & Eslami, F. (2020). Sonophotocatalytic treatment of AB113 dye and real textile wastewater using ZnO/persulfate: Modeling by response surface methodology and artificial neural network. *Environmental Research, 184*, 109367. https://doi.org/10.1016/j.envres.2020.109367

Aziam, R., Chiban, M., Eddaoudi, E., Soudani, A., Zerbet, M., & Sinan, F. (2016). Factors controlling the adsorption of acid blue 113 dye from aqueous solution by dried C. edulis plant as natural adsorbent. *Arabian Journal of Geosciences*, *9*(15), 1–7. https://doi.org/10.1007/s12517-016-2675-4

Aziam, R., Chiban, M., Eddaoudi, H., Soudani, A., Zerbet, M., & Sinan, F. (2017). Kinetic modeling, equilibrium isotherm and thermodynamic studies on a batch adsorption of anionic dye onto eco-friendly dried Carpobrotus edulis plant. *The European Physical Journal Special Topics, 226*(5), 977–992. https://doi.org/10.1140/epjst/e2016-60256-x

Bianchini, G., Marrocchino, E., Tassinari, R., & Vaccaro, C. (2005). Recycling of construction and demolition waste materials: A chemical–mineralogical appraisal. *Waste Management, 25*(2), 149–159. https://doi.org/10.1016/j.wasman.2004.09.005

BOE. Ley 5/2002, de 3 de junio, sobre vertidos de aguas residuales industriales a los sistemas públicos de saneamiento. , Pub. L. No. Ley 5/2002 § 1 (2002). https://www.boe.es/eli/es-as/l/2002/06/03/5. Accessed 9 April 2022

Caicedo, D. F., dos Reis, G. S., Lima, E. C., De Brum, I. A. S., Thue, P. S., Cazacliu, B. G., et al. (2020). Efficient adsorbent based on construction and demolition wastes functionalized with 3-aminopropyltriethoxysilane (APTES) for the removal ciprofloxacin from hospital synthetic effluents. *Journal of Environmental Chemical Engineering, 8*(4), 103875. https://doi.org/10.1016/j.jece.2020.103875

Chen, S., Zhang, J., Zhang, C., Yue, Q., Li, Y., & Li, C. (2010). Equilibrium and kinetic studies of methyl orange and methyl violet adsorption on activated carbon derived from Phragmites australis. *Desalination, 252*(1), 149–156. https://doi.org/10.1016/j.desal.2009.10.010

Damrongsiri, S. (2017). Feasibility of using demolition waste as an alternative heavy metal immobilising agent. *Journal of Environmental Management, 192*, 197–202. https://doi.org/10.1016/j.jenvman.2017.01.052

Debnath, S., & Ghosh, U. C. (2008). Kinetics, isotherm and thermodynamics for Cr(III) and Cr(VI) adsorption from

aqueous solutions by crystalline hydrous titanium oxide. *The Journal of Chemical Thermodynamics, 40*(1), 67–77. https://doi.org/10.1016/j.jct.2007.05.014

Değermenci, G. D., Değermenci, N., Ayvaoğlu, V., Durmaz, E., Çakır, D., & Akan, E. (2019). Adsorption of reactive dyes on lignocellulosic waste; characterization, equilibrium, kinetic and thermodynamic studies. *Journal of Cleaner Production, 225*, 1220–1229. https://doi.org/10.1016/j.jclepro.2019.03.260

Deniz, F., & Saygideger, S. D. (2011). Removal of a hazardous azo dye (Basic Red 46) from aqueous solution by princess tree leaf. *Desalination, 268*(1), 6–11. https://doi.org/10.1016/j.desal.2010.09.043

Dhaif-Allah, M. A. H., Taqui, S. N., Syed, U. T., & Syed, A. A. (2020). Kinetic and isotherm modeling for acid blue 113 dye adsorption onto low-cost nutraceutical industrial fenugreek seed spent. *Applied Water Science, 10*(2), 58. https://doi.org/10.1007/s13201-020-1141-3

Domingues, N. S., Romão, É. L., Alvim, D. S., Marques, J. P., Rodrigues, V. G. S., & Kasemodel, M. C. (2024). Use of Construction and Demolition Waste for the Treatment of Dye-Contaminated Water Toward Circular economy. *Water, Air, & Soil Pollution, 235*(10), 663. https://doi.org/10.1007/s11270-024-07421-w

dos Reis, G. S., Grigore Cazacliu, B., Rodriguez Correa, C., Ovsyannikova, E., Kruse, A., Hoffmann Sampaio, C., et al. (2020). Adsorption and recovery of phosphate from aqueous solution by the construction and demolition wastes sludge and its potential use as phosphate-based fertiliser. *Journal of Environmental Chemical Engineering, 8*(1), 103605. https://doi.org/10.1016/j.jece.2019.103605

Errais, E., Duplay, J., Darragi, F., M'Rabet, I., Aubert, A., Huber, F., & Morvan, G. (2011). Efficient anionic dye adsorption on natural untreated clay: Kinetic study and thermodynamic parameters. *Desalination, 275*(1), 74–81. https://doi.org/10.1016/j.desal.2011.02.031

Esteban-Arranz, A., Pérez-Cadenas, M., Muñoz-Andrés, V., & Guerrero-Ruiz, A. (2021). Evaluation of graphenic and graphitic materials on the adsorption of Triton X-100 from aqueous solution. *Environmental Pollution, 284*, 117161. https://doi.org/10.1016/j.envpol.2021.117161

European Commission. (2008). Directive 2008/98/EC on waste (Waste Framework Directive) - Environment - European Commission. https://ec.europa.eu/environment/waste/framework/. Accessed 31 March 2020

European Commission. (2018). EU Construction and Demolition Waste Protocol and Guidelines. *Internal Market, Industry, Entrepreneurship and SMEs - European Commission*. Text. https://ec.europa.eu/growth/content/eu-construction-and-demolition-waste-protocol-0_en. Accessed 25 March 2020

Eurostat. (2018). Statistics | Eurostat. *Generation of waste by waste category, hazardousness and NACE Rev. 2 activity*. https://ec.europa.eu/eurostat/databrowser/view/ENV_WASGEN__custom_2330979/default/table?lang=en. Accessed 21 March 2022

Gálvez-Martos, J.-L., Styles, D., Schoenberger, H., & Zeschmar-Lahl, B. (2018). Construction and demolition waste best management practice in Europe. *Resources, Conservation and Recycling, 136*, 166–178. https://doi.org/10.1016/j.resconrec.2018.04.016

Garg, V. K., Amita, M., Kumar, R., & Gupta, R. (2004). Basic dye (methylene blue) removal from simulated wastewater by adsorption using Indian Rosewood sawdust: A timber industry waste. *Dyes and Pigments, 63*(3), 243–250. https://doi.org/10.1016/j.dyepig.2004.03.005

Gupta, V. K., Gupta, B., Rastogi, A., Agarwal, S., & Nayak, A. (2011). A comparative investigation on adsorption performances of mesoporous activated carbon prepared from waste rubber tire and activated carbon for a hazardous azo dye—Acid Blue 113. *Journal of Hazardous Materials, 186*(1), 891–901. https://doi.org/10.1016/j.jhazmat.2010.11.091

Hajjaji, W., Pullar, R. C., Labrincha, J. A., & Rocha, F. (2016). Aqueous Acid Orange 7 dye removal by clay and red mud mixes. *Applied Clay Science, 126*, 197–206. https://doi.org/10.1016/j.clay.2016.03.016

Islam, A., Teo, S. H., Taufiq-Yap, Y. H., Ng, C. H., Vo, D.-V.N., Ibrahim, M. L., et al. (2021). Step towards the sustainable toxic dyes removal and recycling from aqueous solution-A comprehensive review. *Resources, Conservation and Recycling, 175*, 105849. https://doi.org/10.1016/j.resconrec.2021.105849

Jain, S. N., & Gogate, P. R. (2017). Acid Blue 113 removal from aqueous solution using novel biosorbent based on NaOH treated and surfactant modified fallen leaves of Prunus Dulcis. *Journal of Environmental Chemical Engineering, 5*(4), 3384–3394. https://doi.org/10.1016/j.jece.2017.06.047

Jiménez-Jiménez, J., Algarra, M., Guimarães, V., Bobos, I., & Rodríguez-Castellón, E. (2017). The Application of Functionalized Pillared Porous Phosphate Heterostructures for the Removal of Textile Dyes from Wastewater. *Materials, 10*(10), 1111. https://doi.org/10.3390/ma10101111

Khalilzadeh Shirazi, E., Metzger, J. W., Fischer, K., & Hassani, A. H. (2020). Removal of textile dyes from single and binary component systems by Persian bentonite and a mixed adsorbent of bentonite/charred dolomite. *Colloids and Surfaces a: Physicochemical and Engineering Aspects, 598*, 124807. https://doi.org/10.1016/j.colsurfa.2020.124807

Kishor, R., Purchase, D., Saratale, G. D., Saratale, R. G., Ferreira, L. F. R., Bilal, M., et al. (2021). Ecotoxicological and health concerns of persistent coloring pollutants of textile industry wastewater and treatment approaches for environmental safety. *Journal of Environmental Chemical Engineering, 9*(2), 105012. https://doi.org/10.1016/j.jece.2020.105012

Lee, L. Y., Gan, S., Yin Tan, M. S., Lim, S. S., Lee, X. J., & Lam, Y. F. (2016). Effective removal of Acid Blue 113 dye using overripe Cucumis sativus peel as an eco-friendly biosorbent from agricultural residue. *Journal of Cleaner Production, 113*, 194–203. https://doi.org/10.1016/j.jclepro.2015.11.016

Li, C., Chen, D., Ding, J., & Shi, Z. (2020). A novel hetero-exopolysaccharide for the adsorption of methylene blue from aqueous solutions: Isotherm, kinetic, and mechanism studies. *Journal of Cleaner Production, 265*, 121800. https://doi.org/10.1016/j.jclepro.2020.121800

Liebau, F. (2003). Ordered microporous and mesoporous materials with inorganic hosts: Definitions of terms, formula

notation, and systematic classification. *Microporous and Mesoporous Materials, 58*(1), 15–72. https://doi.org/10.1016/S1387-1811(02)00546-2

Liu, H., Zhang, J., Li, B., Zhou, N., Xiao, X., Li, M., & Zhu, C. (2020). Environmental behavior of construction and demolition waste as recycled aggregates for backfilling in mines: Leaching toxicity and surface subsidence studies. *Journal of Hazardous Materials, 389*, 121870. https://doi.org/10.1016/j.jhazmat.2019.121870

Mahapatra, M., Karmakar, M., Dutta, A., Mondal, H., Roy, J. S. D., Chattopadhyay, P. K., & Singha, N. R. (2018). Microstructural analyses of loaded and/or unloaded semi-synthetic porous material for understanding of superadsorption and optimization by response surface methodology. *Journal of Environmental Chemical Engineering, 6*(1), 289–310. https://doi.org/10.1016/j.jece.2017.11.078

Márquez, C. O., García, V. J., Guaypatin, J. R., Fernández-Martínez, F., & Ríos, A. C. (2021). Cationic and Anionic Dye Adsorption on a Natural Clayey Composite. *Applied Sciences, 11*(11), 5127. https://doi.org/10.3390/app11115127

Mohan, N., Balasubramanian, N., & Subramanian, V. (2001). Electrochemical Treatment of Simulated Textile Effluent. *Chemical Engineering & Technology, 24*(7), 749–753. https://doi.org/10.1002/1521-4125(200107)24:7%3c749::AID-CEAT749%3e3.0.CO;2-Y

Moreno-Pérez, E., Hernández-Ávila, J., Rangel-Martínez, Y., Cerecedo-Sáenz, E., Arenas-Flores, A., Reyes-Valderrama, M. I., & Salinas-Rodríguez, E. (2018). Chemical and Mineralogical Characterization of Recycled Aggregates from Construction and Demolition Waste from Mexico City. *Minerals, 8*(6), 237. https://doi.org/10.3390/min8060237

Nethaji, S., & Sivasamy, A. (2011). Adsorptive removal of an acid dye by lignocellulosic waste biomass activated carbon: Equilibrium and kinetic studies. *Chemosphere, 82*(10), 1367–1372. https://doi.org/10.1016/j.chemosphere.2010.11.080

Ooi, J., Lee, L. Y., Hiew, B. Y. Z., Thangalazhy-Gopakumar, S., Lim, S. S., & Gan, S. (2017). Assessment of fish scales waste as a low cost and eco-friendly adsorbent for removal of an azo dye: Equilibrium, kinetic and thermodynamic studies. *Bioresource Technology, 245*, 656–664. https://doi.org/10.1016/j.biortech.2017.08.153

Pai, S., Kini, S. M., Narasimhan, M. K., Pugazhendhi, A., & Selvaraj, R. (2021). Structural characterization and adsorptive ability of green synthesized Fe3O4 nanoparticles to remove Acid blue 113 dye. *Surfaces and Interfaces, 23*, 100947. https://doi.org/10.1016/j.surfin.2021.100947

Patel, H. (2018). Charcoal as an adsorbent for textile wastewater treatment. *Separation Sci Technol, 53*(17), 2797–2812. https://doi.org/10.1080/01496395.2018.1473880

Pliatsikas, I., Robou, E., Samouhos, M., Katsiotis, N. S., & Tsakiridis, P. E. (2019). Valorization of demolition ceramic wastes and lignite bottom ash for the production of ternary blended cements. *Construction and Building Materials, 229*, 116879. https://doi.org/10.1016/j.conbuildmat.2019.116879

Porter, J. F., McKay, G., & Choy, K. H. (1999). The prediction of sorption from a binary mixture of acidic dyes using single- and mixed-isotherm variants of the ideal adsorbed solute theory. *Chemical Engineering Science, 54*(24), 5863–5885. https://doi.org/10.1016/S0009-2509(99)00178-5

Prajapati, A. K., Das, S., & Mondal, M. K. (2020). Exhaustive studies on toxic Cr(VI) removal mechanism from aqueous solution using activated carbon of Aloe vera waste leaves. *Journal of Molecular Liquids, 307*, 112956. https://doi.org/10.1016/j.molliq.2020.112956

Prajapati, A. K., & Mondal, M. K. (2020). Comprehensive kinetic and mass transfer modeling for methylene blue dye adsorption onto CuO nanoparticles loaded on nanoporous activated carbon prepared from waste coconut shell. *Journal of Molecular Liquids, 307*, 112949. https://doi.org/10.1016/j.molliq.2020.112949

Reddy, B. S., Maurya, A. K., Narayana, P. L., Pasha, S. K. K., Reddy, M. R., Hatshan, M. R., et al. (2022). Knowledge extraction of sonophotocatalytic treatment for acid blue 113 dye removal by artificial neural networks. *Environmental Research, 204*, 112359. https://doi.org/10.1016/j.envres.2021.112359

Repon, Md. R., Dev, B., Rahman, M. A., Jurkonienė, S., Haji, A., Alim, Md. A., & Kumpikaitė, E. (2024). Textile dyeing using natural mordants and dyes: a review. *Environmental Chemistry Letters*https://doi.org/10.1007/s10311-024-01716-4

Reza Samarghandi, M., Tari, K., Shabanloo, A., Salari, M., & Zolghadr Nasab, H. (2020). Synergistic degradation of acid blue 113 dye in a thermally activated persulfate (TAP)/ZnO-GAC oxidation system: Degradation pathway and application for real textile wastewater. *Separation and Purification Technology, 247*, 116931. https://doi.org/10.1016/j.seppur.2020.116931

Sadeghi, S., Moghaddam, A. Z., & Massinaei, M. (2015). Novel tunable composites based on bentonite and modified tragacanth gum for removal of acid dyes from aqueous solutions. *RSC Advances, 5*(69), 55731–55745. https://doi.org/10.1039/C5RA07979A

Samsami, S., Mohamadizaniani, M., Sarrafzadeh, M.-H., Rene, E. R., & Firoozbahr, M. (2020). Recent advances in the treatment of dye-containing wastewater from textile industries: Overview and perspectives. *Process Safety and Environmental Protection, 143*, 138–163. https://doi.org/10.1016/j.psep.2020.05.034

Santos, D. H. S., Queiroz, L. F., Silva Neto, L. D., Santos, K. E., das Neves, D. D. C. S., Silva, A. F., et al. (2024). Construction and demolition waste as a low-cost adsorbent for water treatment: Kinetics, isotherm, thermodynamics, and Fenton regeneration. *Environmental Science and Pollution Research, 31*(54), 62889–62907. https://doi.org/10.1007/s11356-024-35393-1

Seredych, M., Rodriguez-Castellon, E., Biggs, M., Skinner, W., & Bandosz, T. J. (2014). Effect of visible light and electrode wetting on the capacitive performance of S- and N-doped nanoporous carbons: Importance of surface chemistryhttps://doi.org/10.1016/j.carbon.2014.07.038']

Shirzad-Siboni, M., Jafari, S. J., Giahi, O., Kim, I., Lee, S.-M., & Yang, J.-K. (2014). Removal of acid blue 113 and reactive black 5 dye from aqueous solutions by activated red mud. *Journal of Industrial and Engineering Chemistry, 20*(4), 1432–1437. https://doi.org/10.1016/j.jiec.2013.07.028

Silva, H. J. B. da, Sá, M. L. de, Oliveira, R. S. de, Santos, M. R. M. C., & Matos, J. M. E. de. (2024). Adsorption of methylene blue dye on construction and demolition waste in an aqueous medium. *Cerâmica*, *70*, eWKZU9068. https://doi.org/10.1590/WKZU9068

Silva, V. C., Araújo, M. E. B., Rodrigues, A. M., Cartaxo, J. M., Menezes, R. R., & Neves, G. A. (2021). Adsorption Behavior of Acid-Treated Brazilian Palygorskite for Cationic and Anionic Dyes Removal from the Water. *Sustainability, 13*(7), 3954. https://doi.org/10.3390/su13073954

Solayman, H. M., Hossen, Md. A., Abd Aziz, A., Yahya, N. Y., Leong, K. H., Sim, L. C., et al. (2023). Performance evaluation of dye wastewater treatment technologies: A review. *Journal of Environmental Chemical Engineering, 11*(3), 109610. https://doi.org/10.1016/j.jece.2023.109610

Song, Y., Xu, Q., He, T., Wang, Z., & Yu, L. (2020). Efficient Biodegradation of Azo Dyes Catalyzed by the Anthraquinone-2-sulfonate and Reduced Graphene Oxide Nanocomposite. *ACS Omega, 5*(33), 21137–21144. https://doi.org/10.1021/acsomega.0c02837

Sormunen, P., & Kärki, T. (2019). Recycled construction and demolition waste as a possible source of materials for composite manufacturing. *Journal of Building Engineering, 24*, 100742. https://doi.org/10.1016/j.jobe.2019.100742

Sun, L., Chen, D., Wan, S., & Yu, Z. (2015). Performance, kinetics, and equilibrium of methylene blue adsorption on biochar derived from eucalyptus saw dust modified with citric, tartaric, and acetic acids. *Bioresource Technology, 198*, 300–308. https://doi.org/10.1016/j.biortech.2015.09.026

Tran, H. N., You, S.-J., Hosseini-Bandegharaei, A., & Chao, H.-P. (2017). Mistakes and inconsistencies regarding adsorption of contaminants from aqueous solutions: A critical review. *Water Research, 120*, 88–116. https://doi.org/10.1016/j.watres.2017.04.014

Uddin, M. K. (2017). A review on the adsorption of heavy metals by clay minerals, with special focus on the past decade. *Chemical Engineering Journal, 308*, 438–462. https://doi.org/10.1016/j.cej.2016.09.029

Villen-Guzman, M., Gutierrez-Pinilla, D., Gomez-Lahoz, C., Vereda-Alonso, C., Rodriguez-Maroto, J. M., & Arhoun, B. (2019). Optimization of Ni (II) biosorption from aqueous solution on modified lemon peel. *Environmental Research, 179*, 108849. https://doi.org/10.1016/j.envres.2019.108849

Wang, J., & Guo, X. (2020). Adsorption kinetic models: Physical meanings, applications, and solving methods. *Journal of Hazardous Materials, 390*, 122156. https://doi.org/10.1016/j.jhazmat.2020.122156

Wong, S., Ghafar, N. A., Ngadi, N., Razmi, F. A., Inuwa, I. M., Mat, R., & Amin, N. A. S. (2020). Effective removal of anionic textile dyes using adsorbent synthesized from coffee waste. *Scientific Reports, 10*(1), 2928. https://doi.org/10.1038/s41598-020-60021-6

Yagub, M. T., Sen, T. K., Afroze, S., & Ang, H. M. (2014). Dye and its removal from aqueous solution by adsorption: A review. *Advances in Colloid and Interface Science, 209*, 172–184. https://doi.org/10.1016/j.cis.2014.04.002

Zewde, A. A., Zhang, L., Li, Z., & Odey, E. A. (2019). A review of the application of sonophotocatalytic process based on advanced oxidation process for degrading organic dye. *Reviews on Environmental Health, 34*(4), 365–375. https://doi.org/10.1515/reveh-2019-0024